This article was downloaded by:
On: *25 January 2011*
Access details: *Access Details: Free Access*
Publisher *Taylor & Francis*
Informa Ltd Registered in England and Wales Registered Number: 1072954 Registered office: Mortimer House, 37-41 Mortimer Street, London W1T 3JH, UK

Molecular Crystals and Liquid Crystals
Publication details, including instructions for authors and subscription information:
http://www.informaworld.com/smpp/title~content=t713644168

Analysis of Electro-Optic Characteristics of Polymer-Stabilized Blue Phase Liquid Crystal Driven by In-Plane and Fringe Electric Field

Sukin Yoon[a]; Miyoung Kim[a]; Min Su Kim[a]; Byeong Gyun Kang[a]; Mi-Kyung Kim[a]; Shin-Woong Kang[a]; Seung Hee Lee[a]; Wan Seok Kang[b]; Gi-Dong Lee[b]
[a] Polymer BIN Fusion Research Center, Department of Polymer Nano Science and Technology, Chonbuk National University, Chonju, Chonbuk, Korea [b] Department of Electronics Engineering, Dong-A University, Pusan, Korea

First published on: 11 November 2010

To cite this Article Yoon, Sukin , Kim, Miyoung , Kim, Min Su , Kang, Byeong Gyun , Kim, Mi-Kyung , Kang, Shin-Woong , Lee, Seung Hee , Kang, Wan Seok and Lee, Gi-Dong(2010) 'Analysis of Electro-Optic Characteristics of Polymer-Stabilized Blue Phase Liquid Crystal Driven by In-Plane and Fringe Electric Field', Molecular Crystals and Liquid Crystals, 529: 1, 95 — 101
To link to this Article: DOI: 10.1080/15421406.2010.495683
URL: http://dx.doi.org/10.1080/15421406.2010.495683

PLEASE SCROLL DOWN FOR ARTICLE

Full terms and conditions of use: http://www.informaworld.com/terms-and-conditions-of-access.pdf

This article may be used for research, teaching and private study purposes. Any substantial or systematic reproduction, re-distribution, re-selling, loan or sub-licensing, systematic supply or distribution in any form to anyone is expressly forbidden.

The publisher does not give any warranty express or implied or make any representation that the contents will be complete or accurate or up to date. The accuracy of any instructions, formulae and drug doses should be independently verified with primary sources. The publisher shall not be liable for any loss, actions, claims, proceedings, demand or costs or damages whatsoever or howsoever caused arising directly or indirectly in connection with or arising out of the use of this material.

Mol. Cryst. Liq. Cryst., Vol. 529: pp. 95–101, 2010
Copyright © Taylor & Francis Group, LLC
ISSN: 1542-1406 print/1563-5287 online
DOI: 10.1080/15421406.2010.495683

Taylor & Francis
Taylor & Francis Group

Analysis of Electro-Optic Characteristics of Polymer-Stabilized Blue Phase Liquid Crystal Driven by In-Plane and Fringe Electric Field

SUKIN YOON,[1] MIYOUNG KIM,[1] MIN SU KIM,[1] BYEONG GYUN KANG,[1] MI-KYUNG KIM,[1] SHIN-WOONG KANG,[1] SEUNG HEE LEE,[1] WAN SEOK KANG,[2] AND GI-DONG LEE[2]

[1]Polymer BIN Fusion Research Center, Department of Polymer Nano Science and Technology, Chonbuk National University, Chonju, Chonbuk, Korea
[2]Department of Electronics Engineering, Dong-A University, Pusan, Korea

Downloaded At: 13:36 25 January 2011

Lowering threshold voltage and operating voltage is a critical issue for blue phase liquid crystal (BP LC) because the Kerr constant of liquid crystal mixture is not so high. In order to switch BP LC from optically isotropic to anisotropic state, in-plane electric field should be generated by interdigitated electrodes in general, however, the operating voltage is high and transmittance is relatively low. In this paper, the BP LC driven by fringe electric field is studied as one of the solutions for those problems. Detailed analysis of voltage-dependent characteristics between two devices has been performed.

Keywords Blue phase liquid crystal; Kerr constant; operating voltage; transmittance

Introduction

With the rapid progress of stabilization of blue phase liquid crystals (BPLCs) by polymerizing a mixture of monomers in recent years [1–4], industry's interest in the polymer-stabilized BPLC is rising because of two major advantages of device such as optical isotropy in the dark state and no surface treatment leading to a simplification of a fabrication process [5,6]. Although wide-viewing angle nematic LC devices such as in-plane switching (IPS) [7], fringe-field switching (FFS) [8–10] and vertical alignment (VA) [11,12] modes are mainly applied to LC-television, all devices require alignment of LC in one direction and it is always troublesome especially in large size display.

Address correspondence to Seung Hee Lee, Department of Polymer-Nano Science and Engineering, Chonbuk National University, 664-14 Duchkjin-dong, Cheonju, 561-756, Korea (ROK). Tel.: (+82)63-270-2343; Fax: (+82)63-270-2341; E-mail: lsh1@chonbuk.ac.kr

The optical birefringence of the BP LC is induced by the Kerr effect which is a type of quadratic electro-optic effect caused by electric field induced-reorientation of polar molecules [13] and its relation associated with an applied electric field E can be expressed as an Eq. (1):

$$\Delta n_i = \lambda K E^2 \tag{1}$$

where λ and K are the wavelength and Kerr constant, respectively. Since its refractive ellipsoid has the optical axis along the electric field vector, it has been recognized that the horizontal field-dominant switching modes only can be applicable for the BP LCD device.

At present, IPS and FFS modes are the representative horizontal field-dominant switching modes for nematic LC. For nematic LC, it is generally known that the FFS mode shows higher transmittance and lower operational voltage than those of the IPS mode. In this paper, detail comparison of BPLC devices associated with electrode structure of IPS and FFS modes on voltage-dependant transmittance characteristics has been performed by calculation and experiment.

Downloaded At: 13:36 25 January 2011

Switching Principle and Simulation Conditions

In order to verify the accuracy of simulation tool, we choose two cells, general IPS and FFS type cells. The device configuration of both cells is illustrated in Figure 1. As shown in Figure 1, IPS type cell has electrode pattern width $w = 10\,\mu m$, electrode pattern spacing $l = 20\,\mu m$ and FFS type cell has electrode pattern width $w = 4\,\mu m$, electrode pattern spacing $l = 6\,\mu m$, and thickness of passivation layer $t1 = 0.69\,\mu m$. Both cell structures have electrode thickness $t2 = 0.04\,\mu m$ and cell gap $d = 6\,\mu m$. The LC mixture with cyanophenyl and cyanoterphenyl contains monomer (EHA, Aldrich), reactive mesogen (RM257, Merck), chiral dopants (CB15 and ZLI 4572, Merck) and photo initiator (DMPAP, Aldrich) with proper molar ratio. The LC mixture shows the transition between cholesteric nematic phase – blue phase at 86°C and blue phase – isotropic phase at 92°C. In order to obtain the stabilized blue phase, the cell filled with the solution was irradiated with UV light of $4.7\,mW/cm^2$ during 70 minutes when the LC mixture in blue phase.

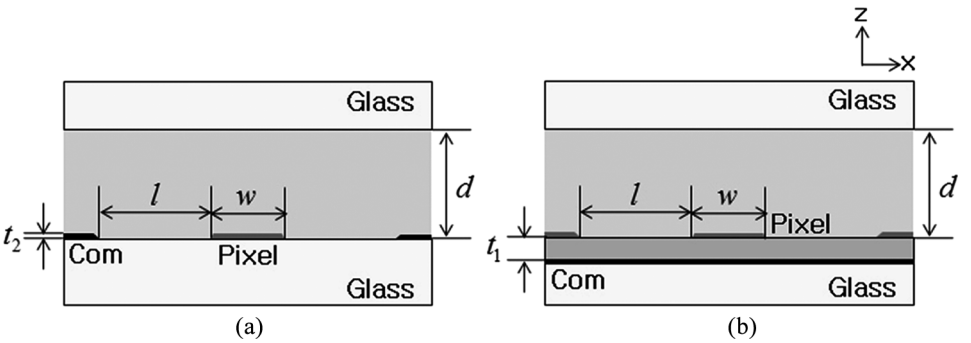

Figure 1. Device configuration of both cells: (a) IPS type cell and (b) FFS type cell.

In the BP LC in which an optically isotropic media exists under crossed polarizer, the transmittance of the device associated with the induced phase retardation described by Eq. (2):

$$T(\lambda) = T_0(\lambda) sin^2\ 2\psi(V) sin^2\ (\pi d_i \Delta n_i(V)/\lambda) \tag{2}$$

where ψ is a voltage-dependent angle between the transmission axes of the crossed polarizers and the induced optical axis of BPLC in XY plane, d_i is thickness of PB LC layer associated with Δn_i and λ is the wavelength of an incident light. In order to have maximum transmission, ψ and $d_i \Delta n_i$ should be equal to 45° and $\lambda/2$ respectively. In other words, the field direction which induces the birefringence should be always 45° with respect to the polarizer.

For the calculation of electro-optic characteristics of two types of BPLC devices, we have employed the commercially available software "TechWiz LCD" (Sanayi system, Korea), which calculates the induced birefringence by Kerr effect as shown in Eq. (1) with an assumption that the induced birefringence of LC mixture cannot exceed a certain maximal birefringence Δn_{max} which is defined by combination of mixture.

Downloaded At: 13:36 25 January 2011

Results and Discussion

The normalized voltage-dependent transmittance (V-T) curves for both IPS and FFS type cells are shown in Figure 2; dots are experimental data measured by spectrometer at $\lambda = 550$ nm and solid lines are simulation results. As shown in Figure 2, a good agreement between the simulation result and the measured data was obtained. Here, for electro-optic simulation, K, Δn_{max} at $\lambda = 550$ nm, and ε_{eff} of

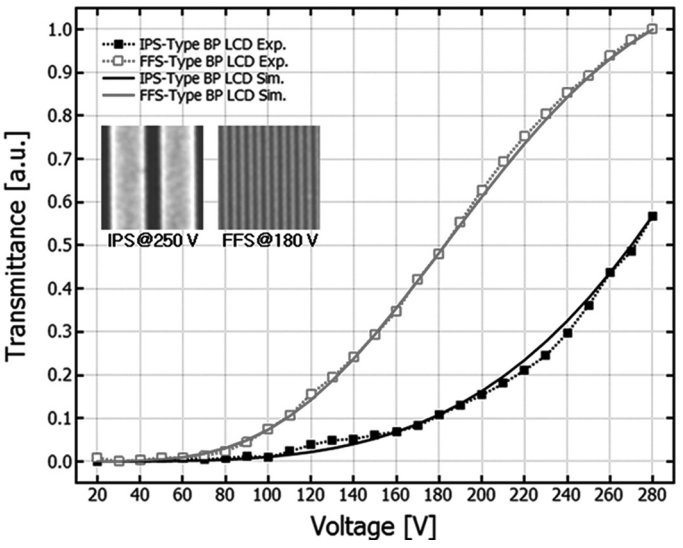

Figure 2. Normalized voltage-dependent transmittance curves for both IPS and FFS type cells (dots are experimental data measured by spectrometer at $\lambda = 550$ nm, images show the operated at 250 V for IPS cell and 180 V for FFS cell).

LC mixture was $2.8 \times 10^{-10}\,\mathrm{m/V^2}$, 0.32, and 24, respectively. The inset images in Figure 2 were taken at an operating voltage of 250 V (for IPS type cell) and 180 V (for FFS type cell), respectively. According to the inset images, IPS type cell showed dark stripe patterns on patterned electrodes, while FFS cell showed dark stripe pattern at the center between the patterned electrodes as well as on patterned electrodes. The reason why FFS type cell showed better performance, even though FFS type cell had dark patterns in two areas (between and on the patterned electrodes), is that IPS type cell has larger length between the patterned electrodes. Therefore, in order to compare the V-T characteristics of IPS and FFS type cells directly, we have employed the same dimensions with electrode pattern width $w = 4\,\mu\mathrm{m}$, electrode pattern spacing $l = 6\,\mu\mathrm{m}$ and cell gap $d = 6\,\mu\mathrm{m}$ for both cells; passivation layer $t_I = 0.3\ \mu\mathrm{m}$ is placed between pixel and common electrode for only FFS type cell. The calculated V-T curves are shown in Figure 3. As we expected, IPS type cell exhibited better transmittance efficiency because it had dark patterns only on the electrodes as shown in inset images in the contrary of FFS type cell. However, although IPS type cell showed better transmittance efficiency, in other V-T characteristics, threshold voltage V_{th} and operating voltage V_{op}, FFS type cell showed lower V_{th} (=38 V) and V_{op} (=246 V) than those of IPS type cell ($V_{th} = 62$ V and $V_{op} = 261$ V), moreover, FFS type cell showed higher transmittance under 170 V.

According to the Eq. (2), in order to maximize transmittance, ψ should be equal to 45° and $d_i \Delta n_i$ should be $\lambda/2$. In this research, ψ was fixed to 45° because we have used stripe patterns, therefore, the transmittance is only related to the phase retardation $d_i \Delta n_i$. Figure 4 shows the induced birefringence Δn_i caused by the horizontal electric field E_x at 150 V. Referring to Figure 4, the induced birefringence Δn_i fully saturated to Δn_{max} only near the patterned electrodes edges and abruptly decreased on the patterned electrodes for both IPS and FFS type cell. At the center area

Downloaded At: 13:36 25 January 2011

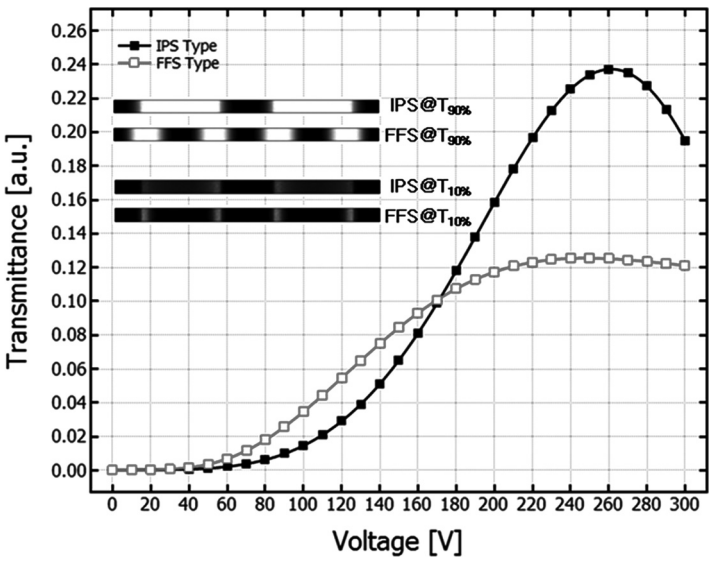

Figure 3. Calculated voltage-dependent transmittance curve (electrode pattern width $w = 4\,\mu\mathrm{m}$, electrode pattern spacing $l = 6\,\mu\mathrm{m}$ and cell gap $d = 6\,\mu\mathrm{m}$ for both cells, images show the operated at 90% and 10% of transmittance of IPS and FFS type cells).

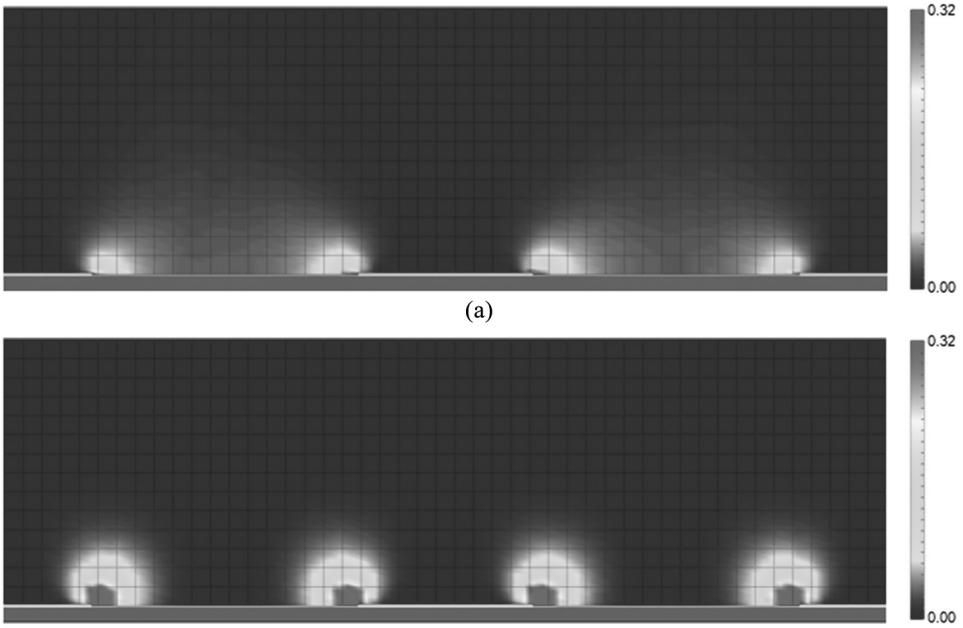

Figure 4. Calculated birefringence induced by the horizontal electric field at 150 V: (a) IPS type cell and (b) FFS type cell.

between the patterned electrodes, IPS type cell exhibited smaller Δn_i than that of near the edges. Although Δn_i was small, since it had broad distribution, it is clear that $d_i \Delta n_i$ seems to reach the $\lambda/2$ phase at higher voltage. On the contrary, FFS type cell showed the abrupt decrease at the center area between the patterned electrodes as well as on the electrodes.

Figure 5 shows the V-T curves of each cell at 5 local regions. According to Figure 5(a), regions B, C, D, and E contributed V-T characteristics in IPS type cell.

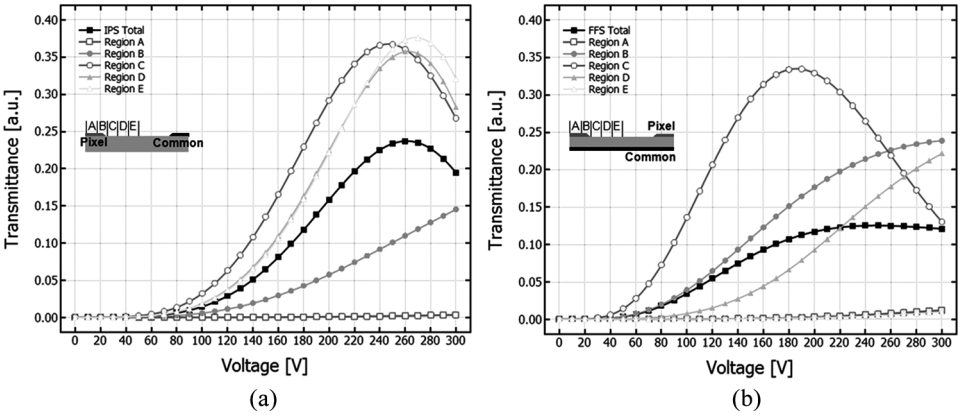

Figure 5. Calculated voltage-dependent transmittance curves at 5 local regions: (a) IPS type cell and (b) FFS type cell.

Downloaded At: 13:36 25 January 2011

Region C exhibited the fastest operation voltage and good transmittance efficiency, and region D and E showed slightly slower operation voltage than that of region C in still good transmittance efficiency, while Region B showed far slower operation voltage than that of region C with lower transmittance efficiency. Region A on the patterned electrodes showed no transmittance at normal direction because only vertical electric field was generated. On the other hand, according to Figure 5(b), regions B, C, and D contributed V-T characteristics in FFS type cell. Similar to what IPS type cell showed, region C exhibited the fastest operation voltage and good transmittance efficiency. However, regions B and D showed big difference, furthermore, region E between the patterned electrodes remained the dark state as well as region A on the patterned electrodes. Referring to Figure 5, the transmittance efficiency was determined by a harmony of local V-T characteristics. Furthermore, region C where locally-strong horizontal electric fields were generated determined the threshold voltage V_{th} and operation voltage V_{op} of cell. Therefore, IPS type cell exhibited the better transmittance efficiency than FFS type cell because it showed good harmony between the patterned electrodes. However, although FFS type cell showed lower transmittance efficiency, its threshold voltage V_{th} and operation voltage V_{op} properties showed better performance.

Downloaded At: 13:36 25 January 2011

Conclusion

In this research, electro-optical characteristics of IPS and FFS type BP LCD have been investigated by numerical simulation. Through numerical simulation, we found that IPS type cell exhibited fully induced birefringence with narrow distribution only near the edges of the patterned electrodes, and smaller birefringence induced broadly along the z-axis between the patterned electrodes. Therefore, although the induced birefringence distribution was non-uniform, the phase retardation by the induced birefringence was comparatively uniform. Contrary to IPS type cell, FFS type cell exhibited fully induced birefringence with thicker distribution near the edges of the patterned electrodes. However, at the center area between the patterned electrodes, only small amount of birefringence was induced. Therefore, as we expected, IPS type cell showed better transmittance efficiency than FFS type cell, however, FFS exhibited better performance under a certain driving voltage because of fully induced birefringence near the patterned electrodes at the low driving voltage.

Acknowledgments

This work was supported by WCU program through MEST (R31-2008-000-20029-0) and partly by Basic Science Research Program through the NRF funded by MEST (2009-0065704).

References

[1] Kikuchi, H., Yokota, M., Hisakado, Y., Yang, H., & Kajiyama, T. (2002). *Nat. Mater.*, *1*, 64.
[2] Hisakado, Y., Kikuchi, H., Nagamura, T., & Kajiyama, T. (2005). *Adv. Mater.*, *17*, 96.
[3] Yoshizawa, A., Sato, M., & Rokunohe, J. (2005). *J. Mater. Chem.*, *15*, 3285.
[4] Choi, S. W., Yamamoto, S. I., Higuchi, H., & Kikuchi, H. (2008). *Appl. Phys. Lett.*, *92*, 43119.

[5] Kikuchi, H., & Higuchi, H. (2007). *SID Tech. Digest*, *38*, 1737.
[6] Ge, Z., Gauza, S., Jiao, M., Xianyu, H., & Wu, S. T. (2009). *Appl. Phys. Lett.*, *94*, 101104.
[7] Oh-e, M., & Kondo, K. (1995). *Appl. Phys. Lett.*, *67*, 3895.
[8] Lee, S. H., Lee, S. L., & Kim, H. Y. (1998). *Appl. Phys. Lett.*, *73*, 2881.
[9] Yu, I. H., Song, I. S., Lee, J. Y., & Lee, S. H. (2006). *J. Phys. D: Appl. Phys.*, *39*, 2367.
[10] Park, J. W., Ahn, Y. J., Jung, J. H., & Lee, S. H. (2008). *Appl. Phys. Lett.*, *93*, 081103.
[11] Takeda, A., Kataoka, S., Sasaki, T., Chida, H., Tsuda, H., Ohmuro, K., Sasabayashi, T., Koike, Y., & Okamoto, K. (1998). *SID Int. Symp. Digest Tech. Papers*, *29*, 1077.
[12] Lee, S. H., Kim, S. M., & Wu, S.-T. (2009). *J. Soc. Inf. Disp.*, *17*, 551.
[13] Haseba, Y., & Kikuchi, H. (2006). *J. Soc. Inf. Disp.*, *14*, 551.

Downloaded At: 13:36 25 January 2011